Malaysian Journal of Catalysis
http://mjcat.utm.my/
MJCat
Research Article

Z-Scheme CoPi/Ag_3PO_4 via Microwave Irradiation for Photodegradation of Rhodamine B

M.S. Azami[1*], N.H. Idris[1], A.H. Nordin[1], K.H. Tan[2], N. Jamaluddin[3], N.I.H. Hazril[4], N.M. Izzudin[4], A.A. Azmi[3]

[1]*Faculty of Applied Sciences, Universiti Teknologi MARA, 02600 Shah Arau, Perlis, Malaysia*
[2]*Centre for Advanced Materials, Faculty of Engineering and Technology, Tunku Abdul Rahman University of Management and Technology, 53300 Kuala Lumpur, Malaysia*
[3]*Faculty of Science, Universiti Teknologi Malaysia, 81310 UTM Johor Bahru, Johor, Malaysia*
[4]*School of Chemical and Energy Engineering, Faculty of Engineering, Universiti Teknologi Malaysia, 81310 UTM Johor Bahru, Johor, Malaysia.*
[5]*UTM Ocean Thermal Energy Centre, Universiti Teknologi Malaysia, Kuala Lumpur 54100, Malaysia*

**Corresponding Author: Tel: +601161717937 (saifulddin@uitm.edu.my)*

Article history:
Received 24 December 2025
Accepted 26 December 2025

ABSTRACT

The widespread use of synthetic dyes in the textile industry has led to severe water pollution, as most dyes are not firmly bound to fabrics and are released into aquatic ecosystems. Unchecked release of untreated dye-bearing effluents critically risks environmental quality and human health. Photocatalytic degradation is considered one of the best and most eco-friendly methods employed to degrade dye pollutants from wastewater. In the present study, a Z-scheme photocatalyst, cobalt phosphate (CoPi) and silver phosphate (Ag_3PO_4), abbreviated as CoPi/Ag_3PO_4, was synthesized by a microwave irradiation method for the photodegradation of Rhodamine B (RhB) dye under visible light. The as-synthesized photocatalysts were characterized by field emission scanning electron microscopy (FESEM), Fourier-transform infrared spectroscopy (FTIR), and UV-visible diffuse reflectance spectroscopy (UV-Vis DRS). The photocatalytic activity was evaluated using a dosage of 0.375 g/L of catalyst in irradiation for 60 minutes. The 5% CoPi/Ag_3PO_4 showed the highest degradation efficiency at 96%, followed by 10% CoPi/Ag_3PO_4 (92%), Ag_3PO_4 alone (87%), 1% CoPi/Ag_3PO_4 (82%), 15% CoPi/Ag_3PO_4 (73%), and CoPi alone (71%). The enhanced activity of 5% CoPi/Ag_3PO_4 was explained in terms of the homogeneous distribution of the Co and P elements on Ag_3PO_4 and the reduced band gap, which favors better absorption and separation of light. Further studies on the effect of different operating conditions, including initial pH, RhB concentration, and catalyst dosage, were conducted. The optimal degradation was achieved at pH 9, 10 mg/L of RhB, and a catalyst dosage of 0.375 g/L. Scavenger experiments indicated that photogenerated holes (h^+) were the major contributors to the mechanism of degradation. Finally, microwave-assisted CoPi/Ag_3PO_4 synthesis is a simple and efficient route to produce visible-light-responsive photocatalysts. Doping CoPi significantly enhanced the photocatalytic activity of Ag_3PO_4, and the composite is a promising material for the degradation of dye-contaminated wastewater

Keywords: *Z-scheme, Photocatalyst, Rhodamine B, Microwave, Silver Phosphate*

| eISSN 0128-2581 |

1. INTRODUCTION

Rhodamine B (RhB) is a xenobiotic group of carcinogens in the body and can increase free radicals. It contains chlorine compounds (Cl-), the CH_3-CH_3, the aromatic micro carbon polycyclic (PAH) Activates the cytochrome enzyme P-450 as well as the very redox structure of the quinone and cause the formation of Reactive Oxygen species (ROS) [1]. RhB waste disposal is a potential threat to marine and terrestrial species, as well as to humans. RhB exposure shortens the length of the estrous cycle in chatty adult females [2]. Follicle atresia and failure to develop can result from a disease called folliculogenesis. As was previously indicated, organic dyes have been subjected to a wide range of treatment strategies. Those techniques, however, have drawbacks like being time-consuming, expensive to produce, and able to produce by-products [3]. As a result, the use of semiconductor photocatalysts in the Advanced Oxidation Process (AOPs) to degrade RhB has attracted widespread attention as a potentially powerful destructive technique for eliminating RhB from the hydrosphere. Ag_3PO_4's narrow band gap and low valence band level make it an effective photocatalyst for oxidizing pollutants. Despite its useful features, Ag_3PO_4 has low photostability because photogenerated electron-hole pairs quickly recombine and Ag ions are rapidly reduced to metallic Ag in the presence of light [4]. Numerous solutions,

such as introducing composite coupling with other semiconductors, have been proposed to address this problem. Composite photocatalysts have the potential to enhance photocatalyst stability, inhibit electron-hole pair recombination, enhance charge carrier separation, and lower surface redox reaction activation energies [5].

According to its abundance on Earth, low cost, photocatalytic properties, and small band gap (2.0 eV), corresponding to the visible light range, cobalt phosphate, CoPi, has recently garnered significant attention from researchers. In addition, some research has shown that adding CoPi to a photocatalyst significantly enhances its ability to oxidize water [6]. To further boost its photocatalytic efficiency, this photocatalyst can also function as a hole collector, reducing the rate at which electron-hole pairs recombine. CoPi/Ag_3PO_4 was first synthesized by Geng et al.,[6] utilizing a one-step hydrothermal process. CoPi/Ag_3PO_4 composite preparation using the traditional approach required at least 24 hours for each sample. This effort will focus on creating a CoPi/Ag_3PO_4 composite photocatalyst employing microwave irradiation for the photodegradation of RhB dye in light of this problem. No investigations on the manufacture of CoPi/Ag_3PO_4 utilizing microwave irradiation, which makes it possible to produce the composite photocatalyst with a quick reaction time and low energy input, have previously been described in the scientific literature [7].

2. EXPERIMENTS

2.1 Preparation of Cobalt Phosphate

The preparation of cobalt phosphate, CoPi, was prepared using the precipitation method. 0.5 g of disodium ammonium phosphate dibasic ($(NH_4)_2HPO_4$) was dissolved in 10 mL of distilled water (solution A). Meanwhile, 1.5 g of cobalt nitrate hydrate $Co(NO_3)_2xH_2O$. $Co(NO_3)_2xH_2O$. was dissolved in 40 mL of distilled water, and the solution was continuously stirred for 30 min (solution B). Solution A was mixed with solution B and stirred for 2 hours. Then, the red precipitation was collected and dried for 4 hours at 110 ℃.

2.2 Preparation of Silver Phosphate

The preparation of silver phosphate (Ag_3PO_4) was prepared using the precipitation method. 0.5 g of disodium hydrogen phosphate anhydrous (Na_2HPO_4) was dissolved in 10 mL of distilled water (solution A). Meanwhile, 1.5 g of silver nitrate ($AgNO_3$) was dissolved in 40 mL of distilled water with continuous stirring for 30 min (solution B). Solution A was mixed with solution B and stirred for 2 hours. Then, the yellow precipitation was collected and dried for 4 hours at 110 ℃.

2.3 Synthesis of CoPi/Ag_3PO_4

The facile solid-state method under microwave irradiation was used to prepare the composite catalyst of CoPi/Ag_3PO_4. The appropriate amount of CoPi and Ag_3PO_4 was mixed in 50 Ml of distilled water. The mixed catalyst was dried for 2 hours at 110 ℃. The dry yellow solid was placed in the microwave for 30 min at 450 W. The CoPi weight loading in the range between 1-15 wt. % were investigated and denoted as x- CP/AP, specifically as 1 CP/AP, 5, CP/AP, 10 CP/AP, and 15 CP/AP.

2.4 Photocatalytic degradation of RhB

The photocatalytic performance of the prepared photocatalysts was compared based on the photodegradation of RhB under visible light irradiation. Photodegradation activity was carried out by suspending 0.03 g of photocatalyst in 25 mL of an aqueous 0.3 mM solution of RhB. This suspension was poured into a glass cell of dimensions 50 mm width × 10 depth × 80 height and irradiated with a 20 W white color LED lamp of irradiance 237 W m-2 with a wavelength between 200-380 nm. An aquarium pump model NS 7200 was used as an aeration source for the supply of oxygen. During each photocatalytic experiment, the decolorization of RhB was determined at specific time intervals until a steady state. The absorbance was measured using an HACH DR 1900 spectrophotometer at 554 nm.

2.5 Characterization

The microscopic surface morphology of the prepared photocatalysts was evaluated through a field-emission scanning electron microscope (FESEM). The optical absorbance was recorded via ultraviolet-visible/diffuse reflectance spectra (UV-Vis/DRS) spectrophotometer and the extrapolation of bandgap photocatalysts. The chemical functional group of the photocatalyst was measured using Fourier transform infrared (FTIR) via the KBr method.

3. RESULTS AND DISCUSSION

3.1 Characterization of photocatalysts

3.1.1 Vibrational spectroscopy

In this study, XRD analysis was performed with the range of 2θ=5- 50° for Al-MCM-41 and 2θ=5-80° for Ni/Al-MCM-41. The diffraction pattern of Al-MCM-41 and Ni/Al-MCM-41 were shown in Figure 1 dan Figure 2. The characteristic peak of the Al-MCM-41 material may be seen in the diffractogram of the material at 2θ=15–30°. This peak suggests the presence of an amorphous phase in the Al-MCM-41 material [20,21]. The impregnated Ni on Al-MCM-41 catalyst exhibits additional peaks at 2θ= 37°, 43°, 62°, and 75° which are associated with the diffraction planes (111), (210) (220), and (311) of face-centered cubic NiO

[22,23]. The presence of the characteristic NiO peak shows that NiO was impregnated successfully on the surface of Al-MCM-41 [4].

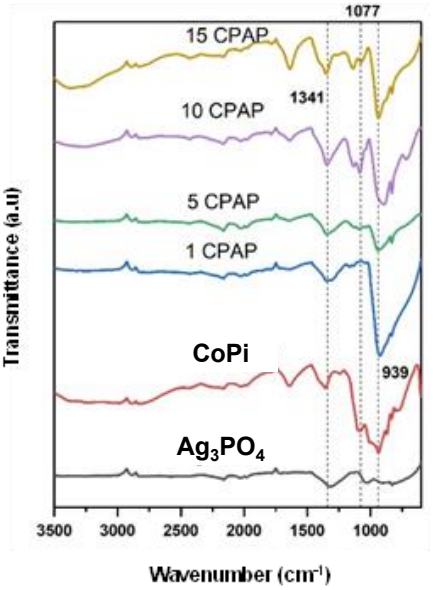

Figure 1. FTIR spectra of synthesized Ag_3PO_4, CoPi, 1 CP/AP, 5 CP/AP, 10 CP/AP and 15 CP/AP with band spectra at 600 – 3500 cm^{-1}

3.1.2 Morphological studies

The surface morphological nature of the prepared photocatalysts was analysed by FESEM micrographs and the recorded images are shown in Figure 2. From the FESEM micrograph, it can be seen that the prepared pure CoPi shows flake-like morphology, while pure Ag_3PO_4 exhibited an irregular shape, as depicted in Figure 2b. The 5 CP/AP sample displays irregular spherical morphology. It was also observed that two components CoPi and Ag_3PO_4, were dispersed well in the hybrids. The well-distributed elements contacted from CoPi on the surface of Ag_3PO_4 are predicted to harvest more visible light that can be absorbed during photocatalytic degradation.

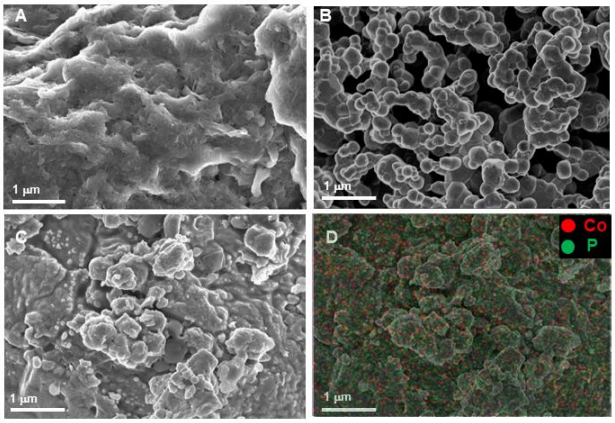

Figure 2. FESEM image of sample (a) CoPi (b) Ag_3PO_4 (c) 5 CPAP, (d) Elemental mapping of sample 5 CPAP showing the spatial presence of Co and P

3.1.3 Optical property studies

The pyridine adsorption FTIR was used to determine the number and kind of acid sites on the catalyst. The pyridine-FTIR spectra of all samples show three adsorption peaks at 1446, 1490 and 1546 cm^{-1} which correlated to Lewis and Brønsted acid sites [25,26]. The adsorption peak at 1446 cm^{-1} was generated due to the transferring electron pairs from the secondary amine group in pyridine to Lewis acid sites in the catalyst. Meanwhile, adsorption at 1546 cm^{-1} correspond to proton transfer from Brønsted acid sites to form a pyridinium ion ($C_5H_5NH^+$) with a pyridine molecule [27]. The adsorption peak at wave number 1490 cm^{-1} associated to the total peak of both Lewis acid and Brønsted acid sites.

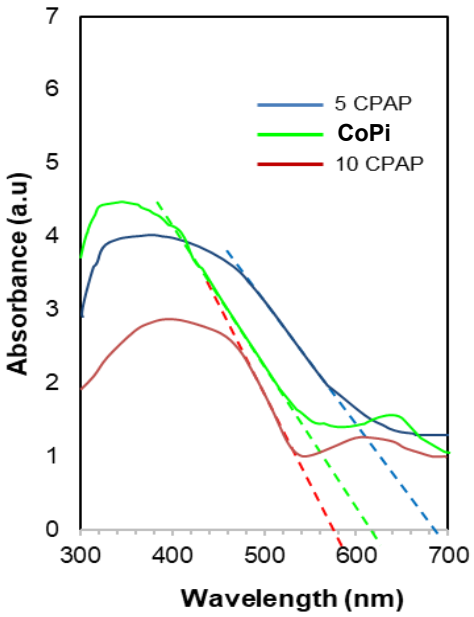

Figure 3. UV-vis diffuse reflectance spectra of the prepared photocatalyst

3.2 Photocatalytic degradation of RhB

The photodegradation of Rhodamine B (RhB) under visible light was used to determine the photocatalytic activity of CP/AP. In order to compare, the identical conditions were used to study the activities of pure CoPi and Ag_3PO_4. As depicted in the Figure 4, when compared to pure CoPi and Ag_3PO_4, all CP/AP catalysts exhibit a greater photocatalytic degradation rate. Since Ag_3PO_4 acts as a supporting catalyst, the composites with CoPi doped in proportions ranging from 1% to 15% demonstrate that the photocatalytic activity differs depending on the ratio. The results of a 60-minute investigation into the CP/AP catalysts'

photocatalytic activity in the breakdown of RhB are illustrated in Figure 4. Evidently, 5 CP/AP degraded at the highest rate (96%) followed by 10 CP/AP (92%), Ag_3PO_4 (87%), 15 CP/AP (73%) and CoPi (71%). The highest performance of 5 CP/AP is owing to the well-distribution element of Co and P on the Ag_3PO_4, which led to high interaction between these two catalysts and reduced band gap energy that will generate more active site and improve the interfacial charge transfer [11].

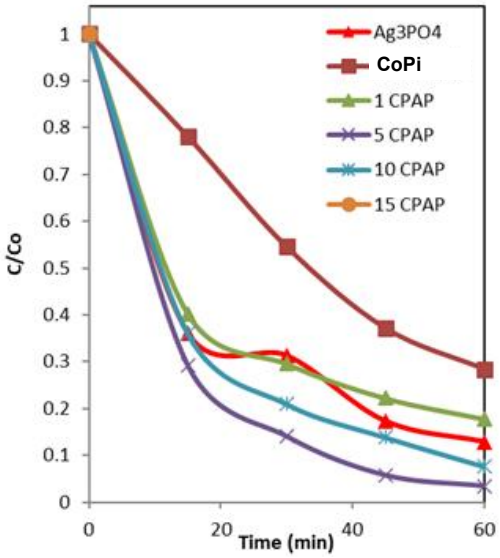

Figure 4. Photodegradation of RhB under visible-light irradiation for the prepared photocatalysts ([RhB] = 10 mg L^{-1}, pH = 6, [catalyst] = 0.0250 g L^{-1}, t = 1 h, 30 ºC)

3.3 Photocatalytic degradation mechanism

Next, the effect of scavenger was performed to determine the role of scavenger species in the photocatalytic mechanism of RhB over 5 CP/AP is shown in Figure 5. The experiment was carried out by using Potassium Iodide (PI), Isopropanol (IP), Methanol (ME) and Potassium Chlorate (PC) as scavenger species for absorbed on the catalyst ($•OH_{surface}$), photogenerated hydroxyl radicals absorbed in the bulk solution ($•OH_{bulk}$) photogenerated holes (h^+) and photogenerated electrons (e-), respectively [12]. Noticeably, Figure 5 indicates that the photogenerated h^+ (66%) played the most crucial role in the photocatalytic decomposition of RhB, followed by photogenerated $•OH_{surface}$ bulk (70%), and $•OH_{bulk}$ (85%). In contrast, the inactive species for 5 CP/AP are photogenerated e- (94%). The above results verified that the interdependent interaction.

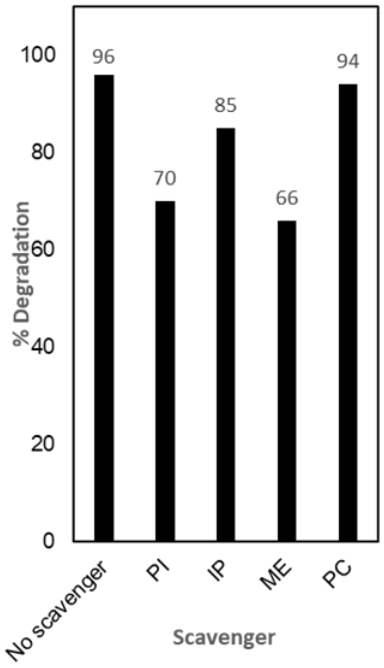

Figure 5. Effect on Scavenger on photodegradation of RhB using 5 CP/AP photocatalyst ([RhB] = 10 mg L^{-1}, pH = 6, [catalyst] = 0.0250 g L^{-1}, t = 1 h, 30 ºC)

Based on the above analysis and discussion, a potential Z-Scheme mechanism of the CP/AP photocatalyst was proposed and schematically illustrated in Figure 6. As the bandgap energy of Ag_3PO_4 has been established in earlier studies [13], it was not re-evaluated here; instead, the reported bandgap value was 2.42 eV, which was used for VB and CB calculations in this proposed mechanism..The photogenerated electrons in the CB of Ag_3PO_4 will recombine with the photogenerated holes in the VB of CoPi, separating the holes in the VB of Ag_3PO_4 and the electrons in the CB of CoPi. Because of its greater negative redox potential than $O_2/•O_2^-$, the electrons in the CB of CoPi have a potential of -0.38 eV, which can create $•O_2^-$. While the holes in the VB of Ag_3PO_4 have a potential of 2.65 eV, they can oxidize H_2O to produce •OH radical because their redox potential is much more positive than the potential level of $H_2O/•OH$ (2.44 eV). Both •OH and h^+ are active radicals that can continually destroy RhB. The internal electric field created by the potent interface between CoPi and Ag_3PO_4 can speed up the recombination of photogenerated electrons in the CB of $Ag_3PO_4$and photogenerated holes in the VB of CoPi. The effective Z-scheme heterostructure preserved with superior oxidic-ability is credited with superior photocatalytic performance.

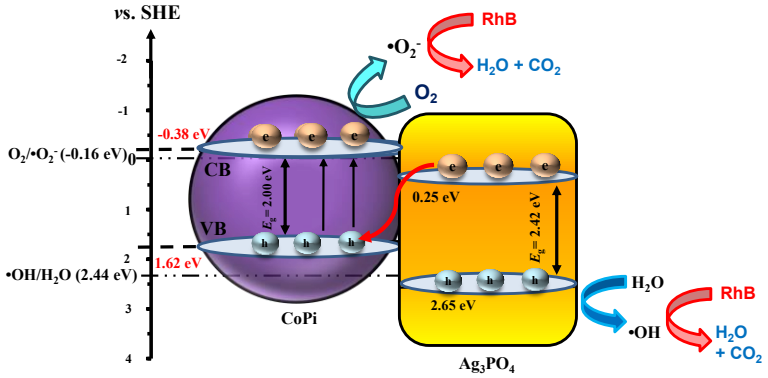

Figure 6. Mechanism of photocatalytic activity of composite CPAP photocatalyst

4. CONCLUSION

In this study, a remarkable enhancement of photocatalytic capability under visible light irradiation was achieved by forming a bulk heterojunction containing CoPi and Ag_3PO_4. This enhancement was ascribed to the efficient charge separation at the heterojunction built between Ag_3PO_4 and CoPi. It is observed that 5 CP/AP serve as the best photocatalyst for degradation of RhB under visible light, with the highest percentage degradation compared to pure Ag_3PO_4 and pure CoPi. The physical and chemical properties of the photocatalysts were examined using FTIR, UV-Vis DRS and FESEM analyses. The results of the characterization show that CoPi was well dispersed on the surface of the Ag_3PO_4. Hence, the bandgap of 5 CP/AP was the lowest compared to others. In addition, 5% CoPi loaded with Ag_3PO_4 shows to be greatly effective in enhancing the photodegradation of RhB activity as compared to pure CoPi, Ag_3PO_4, 1 CP/AP, 5 CP/AP, 10 CP/AP, and 15 CP/AP. This suggests that 5 CP/AP has the best performance in photodegradation of RhB due to its well-dispersed, strong interaction between Co, P and Ag bonds and lowest bandgap. Moreover, the effect of the scavenger shows that the photogenerated h^+ (66%) played the most crucial role in the photocatalytic decomposition of RhB. Then, the mechanism for the photocatalytic activity of RhB was proposed as a Z-Scheme heterojunction. Overall, the CoPi loaded on Ag_3PO_4 successfully contribute on photodegradation of RhB under visible light.

ACKNOWLEDGEMENTS

The authors are grateful for the financial support from the Fundamental Research Grant Scheme- Early Career from the Ministry of Higher Education Malaysia (Grant No. 600-RMC/FRGS-EC 5/3 (056/2024) @ FRGS-EC/1/2024/STG04/UITM/02/16) and Kurita Water and Environment Foundation Research Grant Program 2023 (grant number 4J652).

REFERENCES

1. D. R. Sulistina, S. Martini, Energy Sources, Journal of Public Health Research **9(2)** (2020) 101-104.
2. H. Rohmawati, M. E. Fitriasnani, W. T. Purnani, R. K. Dewi, Journal of Physics: Conference Series **899(1)** (2021).
3. Q. Liu, IOP Conference Series: Earth and Environmental Science **514(5)** (2020).
4. M. S. Azami, A. A.Jalil, F. F. A. Aziz, N. S. Hassan, C. R. Mamat, , A. A. Fauzi, N. M. Izzudin, Separation and Purification Technology, **292** (2022) 120984.
5. A. Amirulsyafiee, M. M. Khan, M. H. Harunsani, Catalysis Communications **172** (2022) 106556.
6. Z. Geng, M. Yang, X. Qi, Z. Li, X. Yang, M. Huo, J. C. Crittenden, Journal of Chemical Technology & Biotechnology **94(5)** (2019) 1660–1669.
7. Q. Hu, Y. He, F. Wang, J. Wu, Z. Ci, L. Chen, R. Xu, M. Yang, J. Lin, L. Han, D. Zhang, Chinese Medicine **16(1)** (2021) 1–22.
8. S. Mandal, R. Ananthakrishnan, ACS Sustainable Chemistry and Engineering **6(1)** (2018) 1091–1104.
9. W. Shi, M . Li, X. Huang, H. Ren, C. Yan, F. Guo, Chemical Engineering Journal 382(2020) 122960.
10. X. Li, , P. Xu, M. Chen, G. Zeng, D. Wang, F. Chen, W. Tang, C. Chen, C. Zhang, X. Tan, Chemical Engineering Journal **366** (2019) 339–357.
11. O.M. Halim, H. Haslinda, , Z. Ahmad, W.I Nawawi, K.H. Tan, Jamaluddin, N, Izzudin, N.M., Jalil, A.A, Azmi, A.A. and Azami, M.S. Malaysian Journal of Chemistry **7(3)** (2025) 38-47.
12. W. Shi, C. Liu, M. Li, X. Lin, F. Guo, J. Shi, Journal of Hazardous Materials 389 (2020).
13. M. S. Azami, A. A. Jalil, W. I. Nawawi, C. R. Mamat, N. M. Izzudin, Materials Today: Proceedings **66(P10)** (2022) 4068–4072.